Proceedings of ITC18, 2008

Recent results of ECRH/ECCD experiments on TCV

F. Felici, E. Asp[1)], S. Cirant[2)] S. Coda, E. Fable, T. Goodman, J. Graves, M. Henderson[3)], J. Paley, F. Piras, O. Sauter, G. Turri, V. Udintsev, C. Zucca and the TCV team

Centre de Recherches en Physique des Plasmas, Association EURATOM-Suisse, École Polytechnique Fédérale de Lausanne, EPFL, 1015 Lausanne, Switzerland
[1)]*EFDA-JET CSU, Culham, United Kingdom*
[2)]*Istituto di Fisica del Plasma, EURATOM-ENEA-CNR Association, Milano, Italy*
[3)]*ITER Organization, Cadarache, F-13108, St Paul-lez-Durance, France*

December 11, 2008

Keywords: ECRH, ECCD, MHD, plasma control, steady-state scenarios, transport barriers

1. Introduction

The Tokamak à configuration variable (TCV) [1] ($B_T <$ 1.5T, R/a = 0.88m/0.25m, $I_p \leq$ 1MA) is located at the Swiss Federal Institute of Technology (EPFL) in Lausanne. It has been conceived primarily as a platform for investigating the effects of different plasma shapes, which can be obtained thanks to a set of 16 independently powered poloidal field coils and an elongated vacuum vessel. This has allowed the study of greatly varying elongation $0.9 < \kappa < 2.8$ and triangularity $-0.6 < \delta < 0.9$.

The auxiliary heating system of TCV is comprised of a 4.5MW EC system [2]. TCV is equipped with 6 gyrotrons providing low-field side launched second harmonic X mode (X2) each 500kW, 82.6GHz and another 3 gyrotrons (500kW, 118GHz each) for top-launched third harmonic X mode heating (X3). The power from each of the X2 gyrotrons is transmitted through windowless transmission lines to a set of six independently steerable launchers. Each launcher has a series of focusing mirrors, of which the final one can move in real-time, adjusting the deposition location in the plasma during a shot. Additionally, the entire launcher assembly can be rotated around the longitudinal axis between shots to change the toroidal injection angle and allow a combination of ECH and co/counter-ECCD to be simultaneously injected in the plasma, both on- and off-axis. By injecting co-ECCD, the plasma current can be sustained non-inductively, using the ohmic transformer only for breakdown and plasma current ramp-up.

The flexibility provided by the X2 EC system is exploited in experiments on subjects such as transport barrier formation [3], [4], [5], current density profile modulation [6], fast electron physics [7], electron transport studies[8], and fully non-inductive, steady-state scenario development [9], [10], [11]. These experiments have contributed to progress in the understanding of physics aspects of EC heated plasmas. A recent, ongoing development is the integration of the ECRH/ECCD system into a digital real-time control system for TCV [12]. This has opened up the possibility for advanced real-time feedback control experiments and will offer increasing opportunities in the future. As ITER will rely on steerable EC launchers for suppression of MHD activity, this is an important line of research.

This paper will focus on several recent results of ECRH/ECCD experiments on TCV. A more complete overview of recent TCV results not specifically related to ECRH/ECCD is provided in [13]. In Section 2, results from real-time control experiments are presented which demonstrate feedback control of the sawtooth period and of the x-ray emission profile peak. Then, an overview is given of results from TCV plasmas featuring electron Internal Transport Barriers (eITBs) (Section 3). Particular attention will be devoted to plasmas with global oscillations. Finally, Section 4 will discuss how tearing modes have been created during off-axis current density profile modulation experiments, suggesting that TCV provides opportunity for studies of classical tearing mode stability and current density profile control .

2. Real-time plasma control using ECRH/ECCD

As mentioned, the angle of the final mirrors of the X2 launchers can be either driven by a feedforward reference or controlled in real-time feedback by the control system. Also the gyrotron power can be controlled in real-time. Previously, the gyrotron power has been controlled in experiments demonstrating the feedback control of ECCD current and global plasma elongation [14]. Recently, an upgraded system has been installed which allows fast ($\sim$ 10kHz) real-time analysis of diagnostic signals and subsequent control actions on local parameters such as magnetic shear[12]. The system is based on dTacq acquisition cards sharing a PCI bus with an embedded computer. Algorithms are designed and tested in

author's e-mail: federico.felici@epfl.ch

Simulink® from which C code is automatically generated and compiled on the target computer. This computer executes analysis/control algorithms and sends command signals to the DACs which control the EC system. The first applications, using the system to control the launcher injection angles, are discussed below.

2.1 Feedback control of the sawtooth period

The sawtooth instability manifests itself in Tokamaks as a periodic sudden decrease in the plasma pressure and temperature inside the $q=1$ surface. It is clearly visible in time traces of central soft X-ray chords and ECE channels as a sawtooth shaped trace. Besides causing a loss of confinement, sawteeth are also known to be possible triggers for Neoclassical Tearing Modes (NTMs) [4] and other MHD activity which may cause disruptions. On the other hand, it is likely that sawteeth will be required in burning plasmas as a mechanism for removing helium from the core [15]. For this reason, it is useful to be able to tailor the sawtooth period, either to stabilize the sawtooth – perhaps to such an extent that the sawtooth period becomes longer than the plasma lifetime– or to destabilize sawteeth, creating more frequent but less perturbing crashes.

It is well known [16] that one of the conditions for the occurence of a sawtooth crash is that the magnetic shear at the $q=1$ surface exceeds a critical limit $s_1 > s_{crit}$. As the core temperature builds up, the current carried in the core increases until the shear exceeds this limit, and the crash is triggered. The shear at the $q=1$ surface can be influenced by localized current injection, either directly by EC current drive or indirectly by local resistivity reduction using EC heating. In past TCV experiments, sweeps of the EC beams across the $q=1$ surface were used to investigate the variation of the sawtooth period, demonstrating that a maximum of the period is found as the beam is close to the $q=1$ rational surface [17]. It should be noted that another important factor determining the sawtooth period is the presence of fast particles, particularly in ICRH heated or burning plasmas [18] but also in NBI heated discharges [19]. However, since TCV does not have a neutral beam injector nor a dedicated ion heating system, fast particles play no role in TCV sawtooth stabilization

In a recent set of experiments, [20] this fact was exploited to control the sawtooth period in feedback. The sawtooth period is determined by analyzing a set of central soft x-ray channels. The period is compared to a requested reference period to generate an error signal which is fed to a controller. This controller moves the mirror of one launcher, which injects 500kW of EC power into the plasma with a combined heating and co-current drive effect. From feedforward sweeps of the mirror position, the response of the sawtooth period to the mirror angle was determined. This dependence, shown in Figure 1, is nonlinear with a clear peak as the deposition location moves from outside to inside the $q=1$ surface. Also, an hysteresis effect can be observed due to the global current density and q-profile modifications as the EC absorption location moves radially. Attention is focused on controlling the sawtooth period while moving the deposition location on the outside of the $q=1$ surface, thus staying on one side of the peak. However, in this region the response is the most nonlinear as can be observed from the increasing slope of the response. This results in an increased gain of the system to be controlled. As is well known from linear control theory [21], using a simple linear controller such as a PID controller may lead to instability if the system gain increases. Reducing the controller gain will however lead to a slow response of the closed-loop system.

In order to be able to obtain different sawtooth periods with the same controller, a nonlinear gain-scheduling controller was designed which moves the mirror at two different speeds depending on the requested sawtooth period. Figure 2 shows the performance and effectiveness of this controller. In the initial phase of the discharge, ECH is turned on with the controller off. The heating location was chosen such that the sawtooth period would increase and exceed the requested period. Then, the controller is switched on and moves the mirror away from the $q=1$ surface to obtain a smaller sawtooth period as requested. After some time, the target period is increased. The mirror then rapidly moves closer to the $q=1$ surface to increase the period. Initially, no change in period is observed due to the mentioned hysteresis effect, however after a while the requested period is obtained and maintained. This provides a demonstration of the possibility to control the sawtooth period in real-time feedback using EC deposition.

2.2 Feedback control of emission profiles

Another application of the real-time feedback of the EC injection angle is the control of profiles in TCV. As the deposition can be steered on- and off-axis simply by pointing the mirror angle towards or away from the plasma center, broader or more peaked profiles can be realised. As TCV lacks a real-time current density profile measurement and the ECE profile is not always straightforward to interpret due to insufficient optical thickness of the plasma, the most readily available diagnostic is the DMPX soft X-ray diagnostic situated at the bottom of the vacuum chamber. It provides good spatial and temporal resolution with 64 lines-of-sight at $<$ 200kHz [22]. All the DMPX channels are read by the real-time algorithm which filters the signals and performs a spline fit to obtain a profile. From the result of the spline fitting, one can derive other quantities – such as the total emission, the peak emission or the relative profile width – any of which can be chosen as control variables.

In a first experiment, the value of the peak emission (defined as the maximum value of the spline fitted profile) was controlled using a single gyrotron and launcher, set to 0° toroidal angle so providing mainly heating. The de-

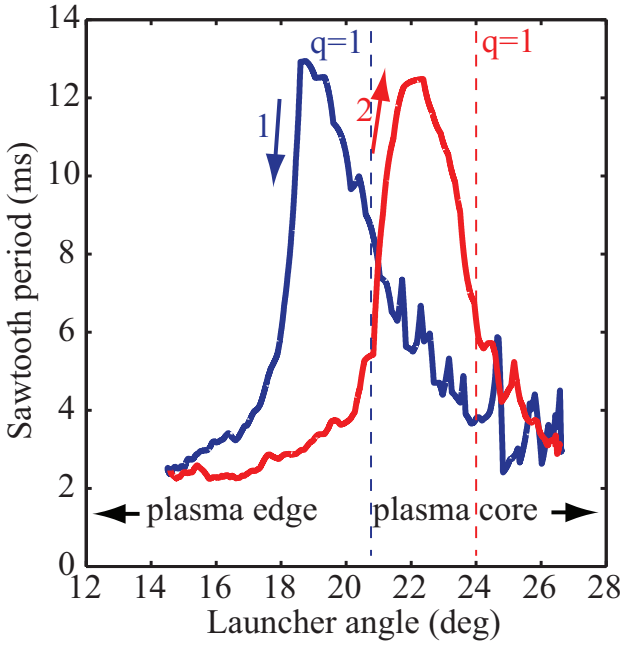

Fig. 1 TCV pulse #35807, Response of the sawtooth period to mirror angle sweep. As the mirror moves across the $q=1$ surface the period peaks and then decays again. The gradient of the curve varies greatly as one approaches the peak. Note that the $q=1$ surface moves during the sweep due to global changes to the current density profile, causing a hysteresis effect.

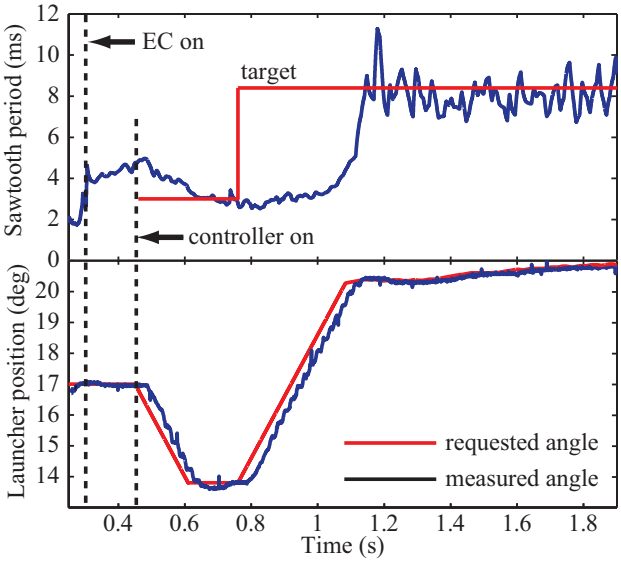

Fig. 2 TCV pulse #35833, demonstrating control of the sawtooth period using a nonlinear, gain-scheduling controller. As soon as the controller switches on the mirror moves to decrease the sawtooth period as is requested. A short time later, the requested period is changed to a higher value. The mirror moves as to move the deposition towards the plasma core in order to increase the sawtooth period. Initially, the period does not change due to the hysteresis effect illustrated in Figure 1.

tected profile peak is subtracted from a reference value and the result is fed into a PI controller. The controller then steers the launcher mirror such that the deposition is closer to the center (to increase the emission peak), or moved off-axis (to decrease it). The controller gains were chosen based on a rough model estimated from a previous pulse where a scan of the mirror angle was done using feed-forward control of the mirror position and were tuned only slightly between experiments. Unlike early tokamak experiments in which the EC *power* was controlled to change the central temperature, the controller here steers the injection angle to achieve the same objective.

Figure 3 demonstrates that the controller successfully obtains two different reference values during the shot. At 0.25s, the gyrotron is switched on while the launcher angle is set at a fixed angle. At 0.4s, the feedback controller is activated and attempts to reduce the peak by moving the deposition location more off-axis. When the reference value is reached, the movement stops. The reference is then increased and the controller responds by moving the launcher back, to provide more central heating. After the control is switched off the peak does not change much since the angle coincidentally stays at a preprogrammed position not far from where it ended up during the feedback control phase.

With these results as a starting point, this methodology will be extended in the next TCV campaign to allow control of several parameters of the emission profiles by varying in real-time the deposition location and power of several gyrotrons.

3. Scenarios with eITBs

Internal electron transport barriers (eITBs) manifest themselves as a marked increase of the core electron temperature and density, resulting in confinement properties superior to L or H modes. Confinement enhancements of 3-6 above the standard L-mode confinement scaling of TCV have been obtained. eITBs are routinely created in TCV discharges in a variety of conditions, including a) fully non-inductive scenarios and b) stationary discharges with a large EC current drive and bootstrap current component, combined with ohmic current [23] [3] [11] [4]. Typically, these plasmas have low density ($\sim 10^{19}\mathrm{m}^{-3}$) and current ($\sim$ 100kA). In previous TCV campaigns, it was demonstrated for the first time unambiguously that the essential requirement for obtaining eITBs is the presence of a negative shear region in the plasma center, and that increasingly negative shear leads to increasing core electron confinement [24]. This was demonstrated by inducing current density profile perturbations with neglibible input power using the ohmic transformer during fully non-inductive scenarios featuring eITBs and it has been confirmed by detailed modeling in [25]. Additionally, precise tailoring of the current and pressure profiles has allowed plasmas to be sustained having 100% bootstrap current in steady

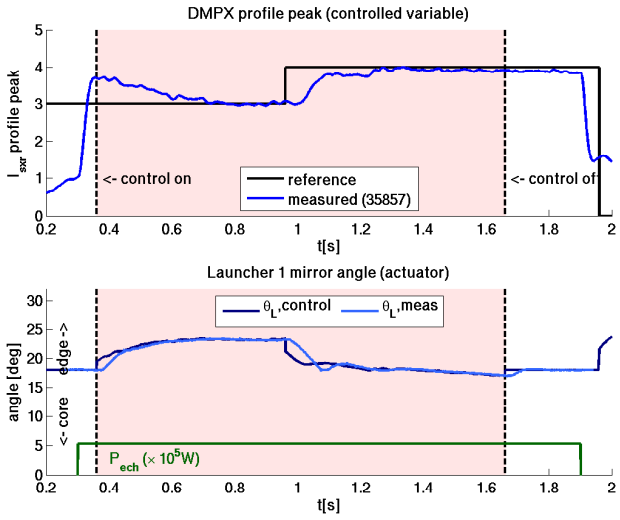

Fig. 3 Control of X-ray emission profile peak. A step reference is given to the controller, which adjusts the mirror angle to obtain more on- or off-axis deposition. The measured mirror angle lags slightly behind the controller reference due to the launcher mechanics and protection filters. The peak traces shown are the result of low-pass filtering and spline fitting of several DMPX channels.

state, lasting over several current redistribution times [26]. Plasmas featuring ITBs are promising candidates for long-pulse steady-state operation in advanced tokamak scenarios as they have a high bootstrap current fraction and good confinement properties. However, these scenarios are often affected by MHD activity, due to the proximity to the infernal stability limit. The interplay between this MHD activity and the eITB can lead to global oscillations of several plasma quantities [5], [27]. In order for ITB scenarios to be applicable to reactor-grade plasmas, such oscillations need to be investigated and methods for their suppression need to be assessed. TCV experiments have focused on these modes and have demonstrated how they can can be suppressed by perturbations of the current density profile.

3.1 Global plasma oscillations

Global oscillations are present in TCV discharges featuring eITBs with strong ECRH/ECCD [5], [27]. These oscillations are caused primarily by the presence of a strong pressure gradient in a region of low magnetic shear. In this case, it can be shown that the eITB plasmas are close to the ideal MHD limit, and so-called *infernal* modes [28] can be triggered. These modes then lead to a confinement degradation and a weakening of the transport barrier. The subsequent reduction of the bootstrap current – which forms a significant part of the total current fraction – leads to a global modification of the current density profile such that the MHD modes are suppressed, the reverse shear region is recovered and the transport barrier is formed again [5]. This cyclic behaviour manifests itself as an oscillation of plasma current, temperature, density and/or radial position, with a frequency of the order of $\sim$10Hz. Depending on the closeness to the ideal limit, the MHD modes may be of resistive (tearing) nature or ideal (crash-like) nature. Similar instabilities have been observed in other Tokamak experiments, notably Tore-Supra, [29] and TRIAM-1M [30]. Recent TCV experiments demonstrated how these oscillations can be suppressed or triggered by modifications of the current density profile.

3.2 Suppression of oscillations using current perturbations

In the experiments described below, eITBs were obtained by strong (typically 1.5MW) off-axis co-ECCD This creates the hollow current density profile required for the formation of the barrier. On-axis heating is also applied to increase the core temperature. Often this central heating is combined with a small counter-current drive component in order to make the current density profile more hollow and the transition more pronounced. Based on this scenario, several methods were tested to perturb the current density profile [27] [5]. The most straightforward perturbation method is the addition of more co-ECCD in the core. In one particular experiment 0.25MW of on-axis co-ECCD was added, effectively making the current density profile less hollow and resulting in a reduction of the barrier and the suppression of the oscillatory regime.

In a second experiment, illustrated in Figure 4, the oscillatory regime was again triggered in a fully non-inductive discharge with 1.5MW of ECCD off-axis and one centrally heating gyrotron with a counter-current drive compoment. This time, however, the co-ECCD power is gradually reduced from 1.5MW to 0.6MW between 1.5s and 2s. In this case, the oscillatory regime is suppressed, but this time it does not lead to a loss of the barrier. The reason for the suppression of the global oscillations has been found by studying the change in q profile due to the change of driven off-axis current. Since TCV does not have a direct measurement of the current density profile, the profiles were modelled by ASTRA [31] transport simulations combined with the CQL3D code [32] to calculate the ECCD current density profile. The result of these simulations is that the q profile minimum is close to 3 (within simulation error bars) in the initial oscillatory phase, but tends to increase as the off-axis ECCD decreases. The main resistive MHD mode (identified as $m/n = 3/1$) is therefore suppressed and the plasma oscillations disappear [27].

The change in ECCD power which causes the suppression of the oscillatory regime not only affects the current density profile, but inevitably also changes the total power deposition. For this reason, a different set of TCV discharges were performed using the ohmic transformer to induce co- or counter current in the plasma. As the plasma conductivity is highest in the center, this perturbation is peaked on axis and significantly affects the reverse shear

responsible for the barrier. It is important to note that ohmic current drive is an order of magnitude more efficient than ECCD, therefore the additional ohmic power is negligible. This experimental method, previously used to prove the link between transport barriers and hollow current density profiles, has also been applied to experiments for suppression of the oscillatory regime [5]. Depending on the sign of the ohmic current perturbation, the plasma can evolve in two different ways. In the case where counter current drive is induced, (making the current density profile more hollow) the barrier strength is increased and the plasma further approaches the ideal MHD limit. In this case, a minor disruption often follows, degrading or destroying the barrier and reducing the confinement. The eITB then recovers with a different q profile which can be oscillation-free. In the opposite case, where co-current drive is induced (making the current profile less hollow) the barrier strength is reduced. This reduces the β_N and the proximity to the MHD limit. The MHD mode is seen to disappear and the plasma maintains good confinement, albeit with a weaker transport barrier. In Figure 5, an example of the latter case is shown. Towards the end of this fully non-inductive discharge, a positive current perturbation (~ 60mV) is added. The low frequency MHD mode, which was initially responsible for the oscillatory plasma behaviour disappears. The central SXR trace shows that the oscillations stop while the barrier is maintained. This is confirmed by comparing Thomson profile measurements before and after the ITB phase [5]. Comparing the case with ECCD (Fig. 4) and ohmic current (Fig. 5) perturbations show that it is indeed the modification of the current density profile which is the key and not the actuators used.

These experiments provide insight into the dynamics of the global plasma oscallations in high-performance eITB scenarios and how they can be avoided. The results suggest that careful tailoring of the current density profile will be necessary in advanced tokamak scenarios in order to maintain a steady-state barrier.

4. Tearing mode triggering by current density profile tailoring

As a final example of the application of ECCD for current density profile modifications in TCV, we illustrate a series of experiments devoted to the modulation of the current density profile. In these so-called Swing-ECCD experiments, two groups of up to three gyrotrons each are set up such as to drive either co- or counter current at the same radial location in the plasma. The power of these two groups is then modulated, one group being on while the other is off. By taking care to carefully align the deposition locations from the different gyrotrons, it was possible to perform experiments modulating the current density profile only, keeping the total injected power constant. The objective of these experiments was to demonstrate the effect of the shear profile on elecron transport. The results of

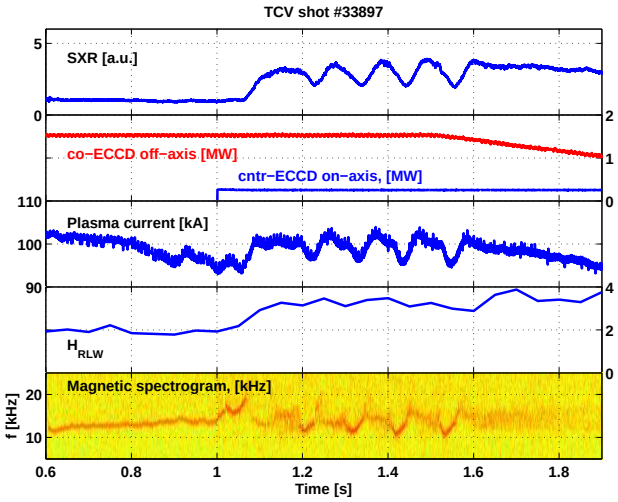

Fig. 4 Perturbation of the current density profile during an eITB discharge by ramp-down of the co-ECCD power combined with counter-ECCD on-axis. The disappearance of the MHD mode is attributed to the dissappearane of the $q = 3$ resonant surface. As can be seen from the SXR measurements, a weaker, oscillation-free barrier remains during the rampdown.

these experiments are detailed in [6] and will not be treated here. During these experiments, however, MHD modes were occasionally visible. These modes are identified as magnetic islands from soft x-ray channel signatures. It is well known that tearing modes can be destabilized classically when Δ' becomes positive [33]. The Δ' parameter depends on the local q profile and its derivatives, which is why local current density perturbations affects the classical tearing stability [34],[35]. Cylindrical tearing stability simulations of the TCV experiments have confirmed that this stabilization or destabilization effect can be achieved with the ECCD injected and it depends on both the direction of the induced current and the location of the current deposition with respect to the rational q surface. It is interesting to perform systematic experiments and comparison with theoretical predictions on the stabilization/ destabilization of tearing modes via localized current drive, not necessarily inside the island as is usually done for tearing mode stabilization and as is forseen in ITER. This should shed further light on the triggering mechanisms determining the onset of tearing modes and methods to prevent and/ or suppress them. These issues will be a focus in coming TCV experiments.

5. Summary and conclusions

This paper has provided an overview of recent experimental results in TCV plamas featuring ECRH/ECCD. Thanks to the localized deposition provided by ECRH or ECCD, many different effects arising from current density and temperature profiles modifications have been studied. Notably, the recent upgrades to the TCV control system have

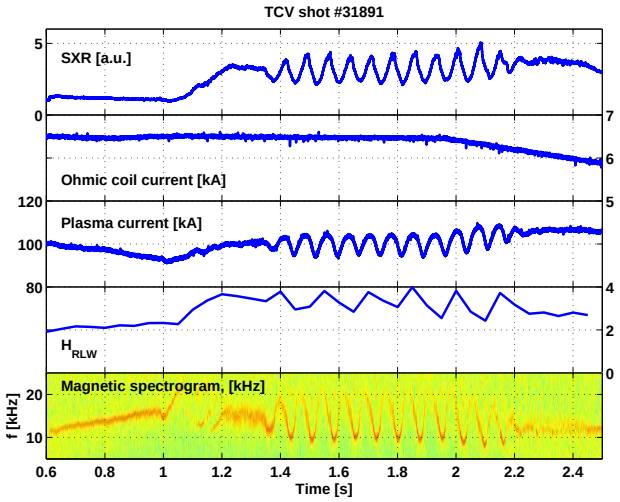

Fig. 5 Perturbation of the current density profile during an eITB discharge by co current induced by the ohmic transformer. The current density profile becomes less hollow, leading to a reduced barrier strength, reduced proximity to the MHD limit and disappearance of the MHD mode responsible for the global plasma oscillations. The gyrotron power does not change throughout the shot.

opened the way to advanced real-time feedback control experiments, demonstrating feedback control of the sawtooth period using a nonlinear controller and preparing the way for further feedback control of both current density and pressure profiles. Much attention has been devoted to scenarios featuring internal electron transport barriers. The fundamental role played by hollow current density profiles in the sustainment of transport barriers has been demonstrated. Furthermore, 100% bootstrap fractions have been achieved in which the bootstrap current profile and the high pressure gradient region are spontaneously well-aligned. In addition, global plasma oscillations often present in high-confinement discharges with eITBs have been studied, revealing that they are intrinsically linked to the appearance of modes due to the proximity to the ideal MHD limit. It has been shown that these modes can be suppressed in a variety of ways by changing the current density profile without necessarily losing the barrier itself. Finally, tearing modes appearing during shear modulation experments indicate that TCV can be a valuable tool for detailed studies of current drive effects on tearing mode stability.

Acknowledgements

This work was supported in part by the Swiss National Science Foundation.

[1] F. Hofmann et al., Plasma Physics and Controlled Fusion **36**, B277 (1994).
[2] T. Goodman and the TCV team, Nuclear Fusion **48**, 054011 (2008).
[3] M. A. Henderson et al., Physical Review Letters **93**, 215001 (2004).
[4] O. Sauter et al., Plasma Physics and Controlled Fusion **44**, 1999 (2002).
[5] G. Turri, V. S. Udintsev, O. Sauter, T. P. Goodman, and E. Fable, Plasma Physics and Controlled Fusion **50**, 065010 (2008).
[6] S. Cirant et al., Modulated ECCD experiments on TCV, in *21th IAEA Fusion Energy Conference*, 2006, Paper EX/P3-3.
[7] S. Coda et al., Nuclear Fusion **43**, 1361 (2003).
[8] Y. Camenen et al., Nuclear Fusion **47**, 510 (2007).
[9] O. Sauter et al., Phys. Rev. Lett. **84**, 3322 (2000).
[10] S. Coda et al., Plasma Physics and Controlled Fusion **42**, B311 (2000).
[11] T. P. Goodman et al., Plasma Physics and Controlled Fusion **47**, B107 (2005).
[12] J. Paley et al., Real time control of plasmas and ECRH systems on TCV, in *IAEA Conference 2008*, 2008.
[13] A. Fasoli, Overview of physics research on the TCV tokamak, in *IAEA Conference 2008*, 2008.
[14] J. I. Paley, S. Coda, and the TCV Team, Plasma Physics and Controlled Fusion **49**, 1735 (2007).
[15] T. Hender et al., Nuclear Fusion **47**, S128 (2007).
[16] O. Sauter et al., Phys. Rev. Lett. **88**, 105001 (2002).
[17] C. Angioni, T. Goodman, M. Henderson, and O. Sauter, Nuclear Fusion **43**, 455 (2003).
[18] J. P. Graves et al., Plasma Physics and Controlled Fusion **47**, B121 (2005).
[19] C. Angioni et al., Plasma Physics and Controlled Fusion **44**, 205 (2002).
[20] J. I. Paley, F. Felici, S. Coda, T. P. Goodman, and F. Piras, Submitted to Plasma Physics and Controlled Fusion (2008).
[21] K. Ogata, *Modern Control Systems*, Prentice Hall, 4th edition, 2002.
[22] A. Sushkov et al., Review of Scientific Instruments **79**, 023506 (2008).
[23] Z. A. Pietrzyk et al., Phys. Rev. Lett. **86**, 1530 (2001).
[24] O. Sauter et al., Physical Review Letters **94**, 105002 (2005).
[25] C. Zucca et al., Plasma Physics and Controlled Fusion **51**, 015002 (2009).
[26] S. Coda, O. Sauter, M. Henderson, and T. Goodman, Fully bootstrap discharge sustainment in steady state in the TCV tokamak, in *IAEA Conference 2008*, 2008.
[27] V. S. Udintsev et al., Plasma Physics and Controlled Fusion **50**, 124052 (2008).
[28] T. Ozeki, M. Azumi, S. Tokuda, and S. Ishida, Nuclear Fusion **33**, 1025 (1993).
[29] G. Giruzzi et al., Phys. Rev. Lett. **91**, 135001 (2003).
[30] K. Hanada et al., (2004).
[31] G. V. Pereverzev, IPP Report 5/42, Max Planck - IPP, 1991.
[32] R. W. Harvey and M. G. McCoy, in *Proc. IAEA TCM/Advances in Simulation and Modeling in Thermonuclear Plasmas*, Montreal, 1992.
[33] H. Furth, P. Rutherford, and H. Selberg, The Physics of Fluids **16**, 1054 (1973).
[34] E. Westerhof, Nuclear Fusion **27**, 1929 (1987).
[35] O. Sauter et al., in *Theory of Fusion Plasmas (Varenna 1998), ISPP-18*, page 403, Bologna, Italy, 1999, Editrice Compositori.